Thermo-mechanical behavior of baritic concrete exposed to high temperature

Francesco Lo Monte, Pietro G. Gambarova *

Department of Civil and Environmental Engineering – DICA, Politecnico di Milano, Piazza L. da Vinci 32, 20133 Milan, Italy

Received 13 January 2014
Received in revised form 26 June 2014
Accepted 12 July 2014
Available online 21 July 2014

1. Introduction

Concrete is generally considered an efficient radiation-shielding material because of its good attenuation properties against X rays, γ rays and fast neutrons, and its mechanical properties, that are hardly affected even under relatively high irradiation levels and neutron fluxes [1]. Such good properties come from the composite microstructure of the concrete, that allows the material to be adapted according to a variety of requirements, and specifically to achieve a good compromise between the mechanical and attenuation properties, without losing the attractive characteristic of being rather inexpensive [2].

Concrete attenuation properties are reached by replacing certain constituents of ordinary mixes and/or by adding new constituents, like replacing the coarse aggregates and adding soluble organic superplasticizers, in order to increase the compactness and to reduce the water content, without impairing the workability. To increase the attenuation properties, dense concretes are used, with heavy aggregates against X and γ rays, and rather light aggregates against fast neutrons [3,4]. In general, if the radiation level is rather low (like in the X-ray chambers of the medical facilities) and the required density is below 3500 kg/m^3, using heavy – and more expensive – concretes should be weighed against using ordinary – and less expensive – concretes, unless the structural problem is controlled by member size. However, concrete densities between 2800 and 3500 kg/m^3 are often adopted, similarly to what is usual in such infrastructures as waste repositories for lightly-irradiated products [5,6].

* Corresponding author. Tel.: +39 02 2399 4391.
E-mail addresses: francesco.lo@polimi.it (F. Lo Monte), pietro.gambarova@polimi.it (P.G. Gambarova).

Among the aggregates used to make concretes heavier, barite (consisting of barium sulphate), corindon (based on aluminium), ilmenite (based on iron and titatium), hematite/magnetite/limonite (based on iron), steel and lead are used, with corindon and hematite being the best in terms of mechanical and thermal properties (high thermal conductivity and low thermal dilation).

To stop fast neutrons, aggregates with high contents of bound water are used, such as those coming from colemanite (calcium borate) and serpentine (containing silicon and magnesium), that are introduced into the mix in the form of sand or gravel. (These aggregates make the concrete similar to ordinary concrete, or even lighter, see Table 1).

As for the cement, all cements characterized by high hydration heat and high shrinkage should be avoided, in order to minimize the thermal stresses in massive members and to avoid – or limit – any subsequent microcracking. Just to give some information on heavy concretes, for a cement content of 350–400 kg/m^3 (Portland/blended/aluminous cement), typical values for the density are:

- 6000–6500 kg/m^3 (with steel scrap, f_c = 75 MPa, w/c = 0.29) [7].
- 5000–5500 kg/m^3 (with colemanite + steel scrap, f_c = 115 MPa, w/c = 0.37) [8].
- 4500–5000 kg/m^3 (with barite + steel scrap or hematite + steel shot, f_c = 35–50 MPa, w/c = 0.31–0.40) [7–15].
- 4000 kg/m^3 (with hematite, f_c = 75–80 MPa, w/c = 0.40) [8].
- > 3500 kg/m^3 (with ilmenite or magnetite, f_c = 75–85 MPa, w/c = 0.30) [7,12,16].
- > 3500 kg/m^3 (with limonite + steel shot, f_c = 60 MPa, w/c = 0.40) [7].
- 3500 kg/m^3 (with barite or magnetite, f_c = 35–45 MPa, w/c = 0.37–0.60) [7,9–15].
- 3000 kg/m^3 (with limonite, f_c = 40 MPa, w/c = 0.50) [7].
- 2800–3000 kg/m^3 (with copper-slag aggregate, f_c = 70–95 MPa; w/c = 0.33–0.45) [17].

As demonstrated by Kan et al. [18], adding iron ore and iron shot (up to 50% of the coarse aggregates) does not affect concrete compressive strength and toughness, but increases the elastic modulus (up to +50%).

The γ-ray irradiation causes the hydrolysis of the free water contained in the concrete, with the expulsion of hydrogen and oxygen, a limited overpressure in the pores, the formation of metastable calcium peroxide and a mass loss [19]. The decomposition of calcium peroxide leads to the production of calcite by combination with carbon dioxide (*carbonation* [3,4,19]). Such carbonation occurs in the bulk of the material and is independent from the natural carbonation along the surfaces. The calcite crystals harden the material, by reducing the size of the pores, as well as by filling the microcracks and the pores caused by the *radiolytic dehydration*. (However, to what extent the porosity is increased or decreased is still an open question).

As for fast neutrons, high fluxes affect the microstructure of quartzitic aggregates, that turns from crystalline to amorphous. Quartz is also subjected to swelling (up to +15% [3]). From the mechanical point of view, however, there is hardly any decay in the concrete exposed to the rather low radiation level of X-ray chambers.

At ambient temperature, both the attenuation properties and the mechanical performance of heavy concretes have been extensively investigated during the last 50 years or more [7–9,16] with a few recent contributions [3,4,13,18], while the information on their mechanical and thermal properties at high temperature (T = 20–750 °C [10,12,17]) is rather limited and needs to be updated, as required by the extension of the service life of several existing nuclear power plants, by the construction of new radioactive-waste repositories and by the increasing awareness of the fire-related risks in medical facilities.

To give an answer to the abovementioned needs, a research project has been recently carried out at the Politecnico di Milano (Milan, Italy) on the high-temperature behavior of a barite-based concrete (target strength f_c^{20} = 30 MPa; nominal mass per unit volume, ρ_c = 3100–3200 kg/m^3 [20]), kept in two different environments to simulate the different behaviors in massive members. In fact, the layers closest to the surface are subjected to dehydration (Mix MD) and those in the core remain relatively moist (Mix MM).

In both cases (three years in air or in moist conditions, after the usual curing for 28 days), a number of cylinders were tested at room temperature and after heating to 5 reference temperatures (T = 105, 250, 400, 550, 750 °C; residual tests) in compression and in tension by splitting. The mass loss, the thermal diffusivity and the porosity were evaluated too, as a function of the temperature (T = 20–750 °C).

Comparisons are made with both ACI and European provisions for ordinary concrete exposed to high temperature, as well as with the *reference* concrete (which is an *ordinary* concrete, Mix M0) tested in a parallel project on the high-temperature behavior of light-weight concretes containing expanded polystyrene synthetized beads [21].

2. Decay at high temperature of ordinary and baritic concretes

There are several factors affecting concrete physical and mechanical properties at high temperature, to the detriment of its overall performance, see for instance Bažant and Kaplan [22]:

- Chemo-physical changes in the hydration products, nano-porosity and bound (*adsorbed*) water.
- Micro-porosity and free-water.
- Thermal compatibility between the aggregate particles and the cement mortar.
- Aggregate chemo-physical stability.
- Additives and admixtures.

Table 1
Chemical composition and main properties of the aggregates used in the concretes aimed to confine X and γ rays, and to stop fast neutrons.

Type	Chemical composition	Mass per unit volume (kg/m^3)	Hardness (Mohs scale)
Hematite	Fe_2O_3	5200–5300	5.0–6.5
Magnetite	Fe_3O_4	5100–5200	5.5–6.5
Ilmenite	$FeTiO_3$	4500–4800	5.0–6.0
Corindon	Al_2O_3	4000	9.0
Barite	$BaSO_4$	3600–4500	3.0–3.5
Colemanite	$2CaO\ 3B_2O_3\ 5(H_2O)$	2950	4.5
Limonite	$FeO\ (OH)\ n(H_2O)$	2700–4300	5.0–5.5
Borocalcite (Howlite)	$Ca_2B_5\ SiO_9\ (OH)_5$	2500–2600	3.5
Serpentine	$Mg_3\ (Si_2O_5)\ (OH)_4$	2500–2600	2.5–4.0

- Thermal transients.
- Stress state (*pre-loading*) during the heating process.

Leaving aside the thermal transients and the stress state (that are related to the structural context and to fire evolution, and not directly to concrete as such), there are factors active at the nano- and micro-level (like the chemo-physical changes in the hydration products, the expulsion of the adsorbed and free water, the aggregate stability, the additives and the admixtures) and factors active at the meso-level (like aggregate-cement thermal compatibility). Since all the previously-mentioned factors play in principle similar roles in both ordinary and baritic concretes, the question is: why should baritic concrete behave differently from ordinary concrete – and particularly from limestone or calcareous concrete – at high temperature?

The answer should take care of three pluses and two minuses characterizing baritic concrete:

- Barite as a mineral is chemically stable (melting temperature = 1580 °C).
- Medium/coarse baritic aggregates and baritic mortar (*hydrated cement + baritic fines*) have rather close coefficients of thermal expansion (Fig. 1a and b) and thermal elongations (Fig. 1c), to the advantage of their kinematic compatibility at any temperature [11]. (Note that in Fig. 1a the cloud envelopes the values of limestone thermal coefficient that are different along the three crystallographic axes).
- Barite as a mineral has a highly-microfractured structure, which makes the material rather soft (and certainly not among the best aggregates), but increases concrete creep at any temperature (Fig. 2: $T = 20$ and 300 or 450 °C), to the advantage of the kinematic compliance among concrete components [11].

However:

- Barite microfractured structure brings in intersecting surfaces, that act as preferential paths in favoring the splitting of the rock particles [9].
- The microfractures are either empty or partially/totally filled with baritic powder, iron oxides and clay containing small amounts of chalcedony, quartz and zeolites, the last three products being rather heat sensitive [9,23], because of the crystallization water they contain and that is expelled at 200–500 °C.

With reference to the thermal compatibility, in the range $T = 150–350$ °C limestone aggregate-LA dilates always less than limestone mortar-LM ($[\alpha_{th}(LA)/\alpha_{th}(LM)]_{AV} = 0.73$), while in a similar range ($T = 200–400$ °C) the thermal dilations of baritic aggregate-BA and baritic mortar-BM are rather close ($[\alpha_{th}(BA)/\alpha_{th}(BM)]_{AV} = 1.08$). So, whether the pluses and the minuses counterbalance each other at high temperature is an open question, that this project is trying to answer.

3. Mix design and compressive strength of the virgin materials

The constituents as well as the main physical and mechanical properties of the concretes investigated in this project are summarized in Table 2. Two nominally-identical mixes called MM (= aging for three years in moist conditions) and MD (= aging for three years in dry or ordinary conditions) were investigated.

Three other mixes are reported as well in Table 2: Mixes CE, SE and M0, where CE stands for the mix design suggested for baritic concretes by the Corps of Engineers (1963 [7]), SE stands for the baritic mix design tested by Sakr and El-Hakim (2005 [12]), and M0 is a *reference* mix tested in Milan in a companion project on light-weight concretes containing expanded polystyrene

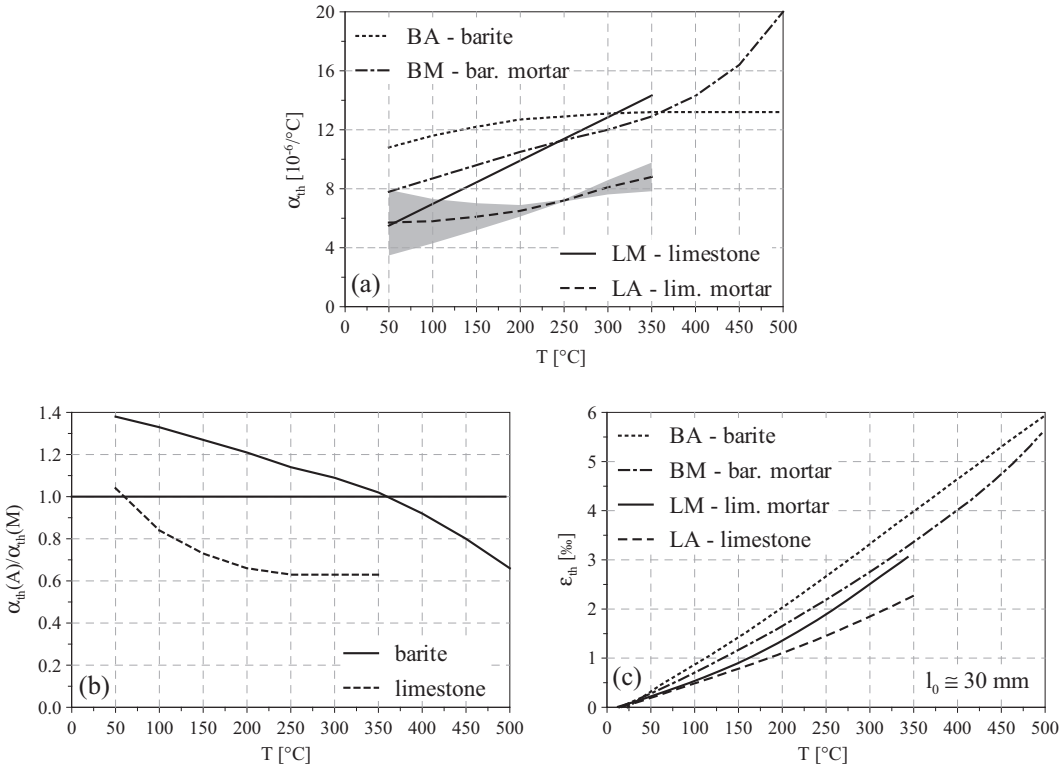

Fig. 1. (a) Plots of the coefficients of thermal expansion of mortars and aggregates; (b) normalized plots of the thermal coefficients (A = aggregate; M = mortar); and (c) plots of the thermal strain, as a function of the temperature (adapted from Crispino [11]).

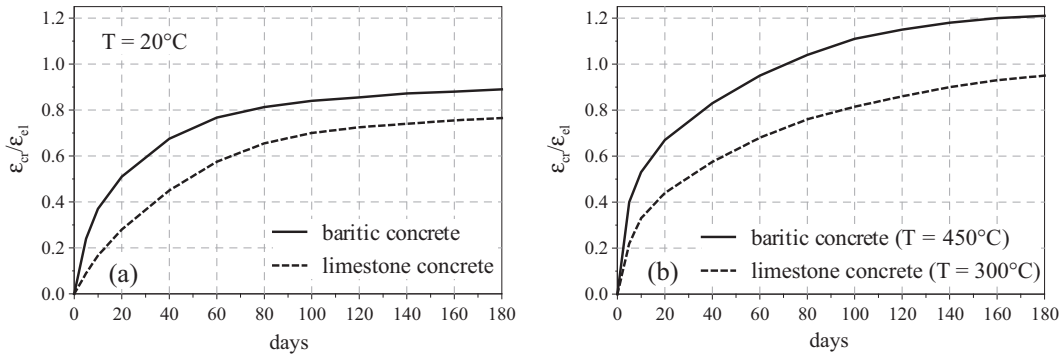

Fig. 2. Plots of the creep coefficients for limestone and baritic concretes at $T = 20$ °C (a); and $T = 300$ or 450 °C (b), as a function of load duration (adapted from Crispino [11]).

Table 2
Mix design, mass per unit volume and mechanical properties of two baritic mixes from the literature (CE and SE), of the *reference* ordinary mix (M0) and of the baritic mixes investigated in this study (MM and MD, cured in *moist* and *dry* conditions, respectively).

Concrete mix	CE (1963)	SE (2005)	M0-Ref.	MM-moist	MD-dry
Cement type – [c (kg/m^3)]	C-I [406]	C-I [400]	C-II-A 42.5 N [286]	C-II-B 42.5 N [340]	C-II-B 42.5 N [340]
BA – Baritic aggregate: Size (mm)	0–37.5	0–20	–	0–25	0–25
BA – Mass per unit volume (kg/m^3)	4500	4000	–	4000	4000
BA – Content (kg/m^3)	3022[e]	2746[f]	–	2500	2500
Sand – siliceous + gravel – mixed 0–20 mm (kg/m^3)	–	–	796 + 989	–	–
Fine/medium aggr. – mixed 0–8 mm (kg/m^3)	–	–	–	174	174
Water added to saturate the aggr. (kg/m^3)	–	–	30	30	30
Effective water (kg/m^3) [w/c]	198 [0.49]	160 [0.40]	200 [0.70]	170 [0.50]	170 [0.50]
Plasticizer/superplasticizer – p/sp (kg/m^3) {p/c}[sp/c]	4.1 {1%} Adipic acid	2.5 [0.6%] Sikament 163	3.9 [1.4%] Acrylic	1.7 [0.5%] Polycarboxylate	1.7 [0.5%] Polycarboxylate
Nominal mass/actual mass per unit volume (kg/m^3)	3630/–	3308/3250[a]	2309[g]/2239[b]	3216/3104[c]	3216/3059[c]
Entrapped air by vol./moist. content by mass (%)[d]	–	–	–/3.1[b]	2.0/3.4[c]	2.0/1.4[c]
Cylinder strength f_c (MPa)	25[a]	47[a]	25.8[b]	27.4[c]	34.6[c]
Secant modulus E_c (GPa) – $\sigma_c \leqslant f_c/2$	–	29[a]	23.3[b]	24.6[c]	26.3[c]

All aggregates in water-saturated surface-dry conditions, unless otherwise specified.
[a] 28 days.
[b] 90 days.
[c] 3 years after casting.
[d] Measured after two weeks at 105 °C.
[e] Fine aggr. = 43% = 1350 kg/m^3 ($d_a \leqslant 3.5$ mm); coarse aggr. = 57% = 1800 kg/m^3 ($6.4 \leqslant d_a \leqslant 37.5$ mm).
[f] Fine aggr. = 45% = 1236 kg/m^3 ($d_a \leqslant 5.0$ mm); coarse aggr. = 55% = 1510 kg/m^3 ($5.0 \leqslant d_a \leqslant 20.0$ mm).
[g] Including 3.9 kg/m^3 of viscosity modifier.

synthetized beads [21]. Note that: (a) the compressive strengths of Mixes CE, SE and M0 (25, 39 and 26 MPa) are rather close to those of Mixes MM and MD (27 and 35 MPa); (b) Mix CE is definitely heavier (3630 kg/m^3) than Mixes SE, MM and MD (close to 3200 kg/m^3); and (c) Mix M0 – being a *reference* mix for ordinary concrete – is lighter than the other mixes (close to 2250 kg/m^3). Also, Mixes MM and MD are very similar to the *optimal* mixes suggested in [7,8,14,15] with w/c = 0.30–0.50 and $c \geqslant 350$ kg/m^3; however, lower cement contents and higher water/cement ratios are often found in the literature [9,10,13]. Mixes MD and MM were meant to represent (a) the loss of water at the fresh state and the dehydration of the outer layers in massive members (Mix MD), and (b) the nearly sealed conditions of the inner layers in the curing and aging phases (Mix MM).

The specimens were cured for 28 days in controlled conditions ($T = 22$ °C and R.H. $\geqslant$ 95%); then Mix MM was kept for three years (2010–2012) in the same controlled environment, while Mix MD was exposed for three years to normal ambient conditions ($T = 20$–25 °C, R.H. = 70–80%), before testing. As for Mix M0, two months in air followed the usual 28 days of curing in controlled conditions.

While six *reference temperatures* were investigated for Mixes MM and MD ($T = 20$, 105, 250, 400, 550, 750 °C), only five temperatures were considered in the case of Mix M0 ($T = 20$, 150, 300, 500, 700 °C).

4. Specimens, thermal cycles and instrumentation

For both Mixes MM and MD, twelve cylinders were cast ($\varnothing = 100$ mm, $h = 300$ mm); all were cut in order to have a first cylinder for testing in compression ($\varnothing = 100$ mm, $h = 200$ mm) and a second cylinder (called *disk* in the following) for testing in indirect tension by splitting ($\varnothing = 100$ mm, $h = 80$ mm). In this way 48 specimens were available (48 = 2 mixes × 6 temperatures × 2 test modalities × 2 specimens for repeatability, Fig. 3a and b).

For each mix, one cylinder was instrumented with two thermocouples to evaluate the thermal diffusivity up to 750 °C. After cooling down to room temperature, this cylinder was tested as well, since it had reached the reference temperature of 750 °C.

The displacement-controlled tests in compression were carried out by means of an electromechanical press Schenck (capacity 1000 kN). The shortening of the specimens was measured via 3 strain transducers placed at 120° astride the mid-height section (base length 50 mm); moreover, 3 LVDTs measured the platen-to-platen distance of the press to monitor the post-peak behavior of the specimens.

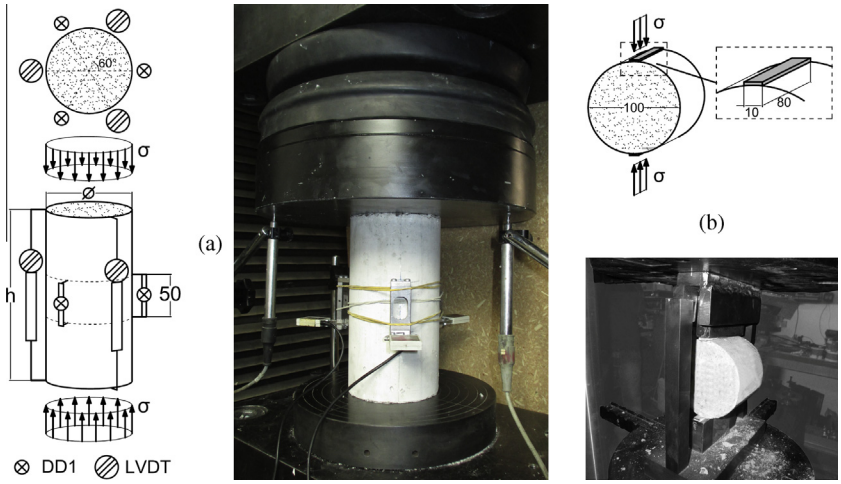

Fig. 3. Typical specimen ready to be tested in compression (a); and in indirect tension (b). The top platen is connected to a self-blocking spherical head.

In all the tests in compression, stearic acid was smeared on the end sections of the specimens to reduce the platen-to-concrete friction. All the tests on disks subjected to tension by splitting were force controlled and an electromechanical press INSTRON was used (capacity 100 kN).

Reference was made to the European Standard EN 12390-6 (2009 [24]), with all the dimensions of the cylinders and of the packing strips scaled down by 1/3 compared to typical specimens ($\varnothing$ = 150 mm; $L/\varnothing \geqslant 1$ or = 2 for cast or cored specimens, respectively), as shown in Fig. 3. However, the value of the ratio $L/\varnothing$ was limited to 0.8, as each 300 mm-long cast specimen had to be cut in two parts to form a 200 mm-cylinder and a 80 mm-disk for the tests in compression and in tension by splitting.

The elastic modulus was evaluated from the stress–strain curves in compression, as *secant modulus* ($\sigma_c \leqslant 0.5 f_c$). Prior to being tested, all specimens were subjected to ultrasounds to measure the velocity of the longitudinal waves (v_{us}), that decreases with the temperature and is instrumental in formulating a *damage index*, as mentioned in the last chapter before the conclusions.

All specimens were slowly heated to the reference temperature (heating rate = 1 °C/min) and rested at that temperature for two hours, to guarantee the chemo-physical uniformity of the material. Then, the specimens were slowly cooled down to 200 °C in controlled conditions (cooling rate = 0.25 °C/min) and to 20 °C in natural conditions (inside the closed furnace), Fig. 4a. Note that the limited number of the specimens (two per each reference temperature and mix) does not diminish the reliability of the results, since in all cases the repeatability of the tests was excellent (see the case of Mix MD in Fig. 4b).

5. Moisture content and mass per unit volume

The specimen tested in compression in virgin conditions (T = 20 °C) were placed inside an oven at 105 °C for two weeks, in order to measure the stabilized mass after the loss of the free water, see Fig. 5a. (The underlying assumption is that previous cracking can hardly modify moisture content). Of course, prior to heating the finest debris were brushed away.

For both MM and MD mixes, mass stabilization was reached in one week, with a normalized moisture loss close to 3.4% and 1.4%, respectively. A similar behavior was observed in the case of mix M0, whose moisture loss (3.1%) was very close to that of mix MM (3.4%), because the former mix had been left in air for a limited period of time (60 days).

As for mass evolution at higher temperatures, all specimens to be tested in compression were weighed before and after each thermal cycle. The average mass loss (measured on two specimens for each reference temperature and mix) is plotted in Fig. 5b for the three mixes. The mass loss of the heavy mixes (MM and MD, close to −5% at 750 °C) is slightly smaller than that of the reference mix (M0, −7.5% at 700 °C), which is in perfect agreement with the normalized mass loss predicted by EC2 – fire design for ordinary concrete (see the continuous curve in Fig. 5b [25]).

6. Porosity

The porosity was investigated by means of two well-known techniques, Mercury Intrusion Porosimetry (MIP) and Water

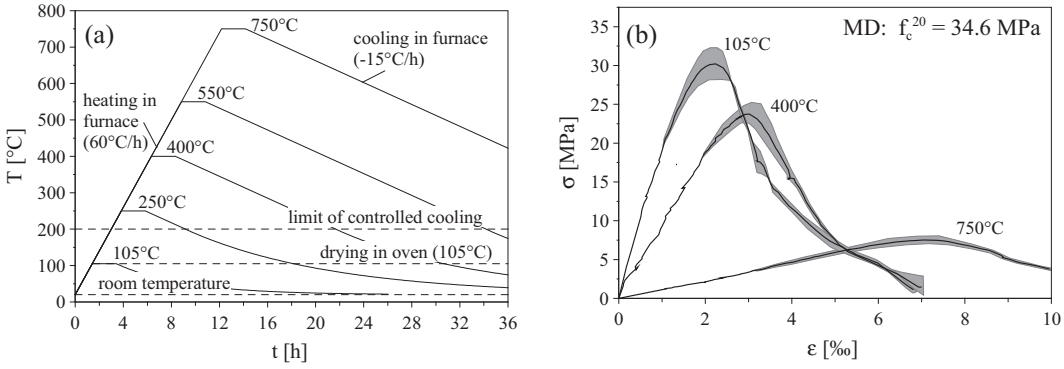

Fig. 4. Thermal cycles (a); and typical dispersion of the test results (b).

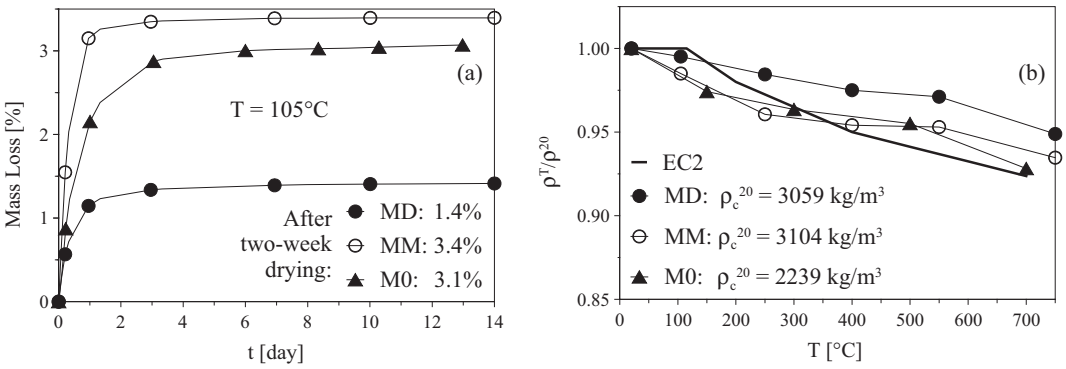

Fig. 5. Mass decrease due to free-water expulsion, at 105 °C, as a function of time (a); and mass loss at high temperature as a function of the temperature (b).

Absorption Porosimetry (WAP), in virgin conditions (T = 20 °C) and after heating to 250, 550 and 750 °C (Mixes MM and MD) or to 300 and 600 °C (Mix M0). For each mix and temperature, small cylinders (Ø = 25 mm; h = 20 mm) were cored from the two halves of the specimens used in the splitting tests, to measure the porosity by means of MIP (Technical Document Norm 4/80 of the Italian Council for Research – CNR, 1980). Later, small quantities of concrete were got from the remaining halves, to be examined by means of WAP (T.C. ISO 5017:1998). Both techniques allow to evaluate the total porosity, but the former gives also information about the pore-size distribution. Preliminarily, the specimens were desiccated in a oven at 105 °C.

Before looking at the evolution with the temperature, one should remember that WAP generally yields higher values than MIP in terms of total porosity because of the small size of the water molecules, which penetrate more easily into the pores, and specifically into the nanopores. For the three mixes, the total porosity evaluated by means of MIP (Fig. 6a) increases regularly with the temperature and – as expected – is lower than the porosity measured by means of WAP (Fig. 6b), at any temperature. Summing up, in spite of barite microfractured nature, the two baritic concretes examined in this project have a porosity that is hardly different from that of a typical ordinary concrete. As for pore-size distribution, in all mixes there are two peaks at any temperature (Fig. 7a–c).

In Mix M0 (Fig. 7a), most of the pores at 20 °C are comprised between the two peaks (30 and 300 nm), while at 600 °C pore size goes from 60 nm to 4 μm, with a remarkable increase of the mean pore size. A similar behavior is exhibited by the heavy mixes, where pore size increases as well, but to a much lesser degree, from 40–400 nm at 20 °C to 60–500 nm at 750 °C in Mix MM, and from 30–200 nm at 20 °C to 60–400 nm at 750 °C in Mix MD.

7. Thermal diffusivity

The thermal parameter controlling heat transmission by conduction in steady or quasi steady conditions is the thermal diffusivity, that is the ratio between the heat transmitted and the heat stored by the unit mass of the material in question. (The larger the thermal diffusivity, the lower the insulation ability).

The thermal diffusivity is defined as: $D = \lambda/(c\rho)$, where λ is the thermal conductivity, c is the specific heat and ρ is the mass per unit volume. In a long cylinder ($h \geqslant 2\varnothing$) subjected to a constant heating rate (v_h = mean heating rate inside the specimen, according to [26]), the thermal diffusivity can be evaluated by means of the following equation:

$$D = v_h R^2/(4\Delta T) \quad (1)$$

where $\Delta T = T_2 - T_1$ is the difference between the temperatures measured in two points (at – or close to – the surface and along the axis, both in the mid-span section), while R is the distance between the two points (Fig. 8a).

Three cylinders – one for each mix – were instrumented with 2 thermocouples and slowly heated from 20 to 750 °C (Mixes MM and MD), and to 700 °C (Mix M0); T_1 and T_2 were measured at regular intervals.

As shown in Fig. 8b, between 200 and 550 °C the thermal diffusivity of Mixes MM and MD is roughly constant (= 0.38–0.30 mm^2/s), but Mix MM always shows a slightly lower diffusivity, because of its larger amount of free and bound water. On the whole, the thermal diffusivity of the two heavy mixes is slightly underevaluated by the equations presented in EC2, provided that the thermal conductivity and the specific heat are those of ordinary concrete and the mass per unit volume is that of the baritic concrete

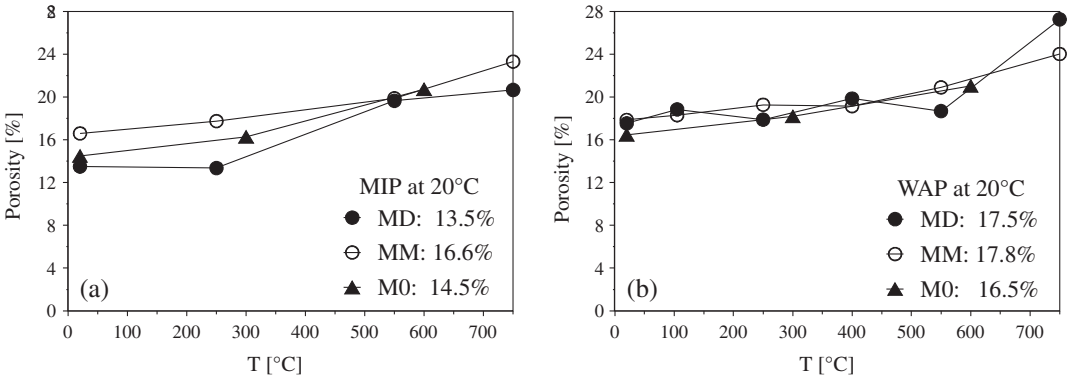

Fig. 6. Plots of the porosity according to Mercury Intrusion Porosimetry – MIP (a); and to Water Absorption Porosimetry – WAP (b).

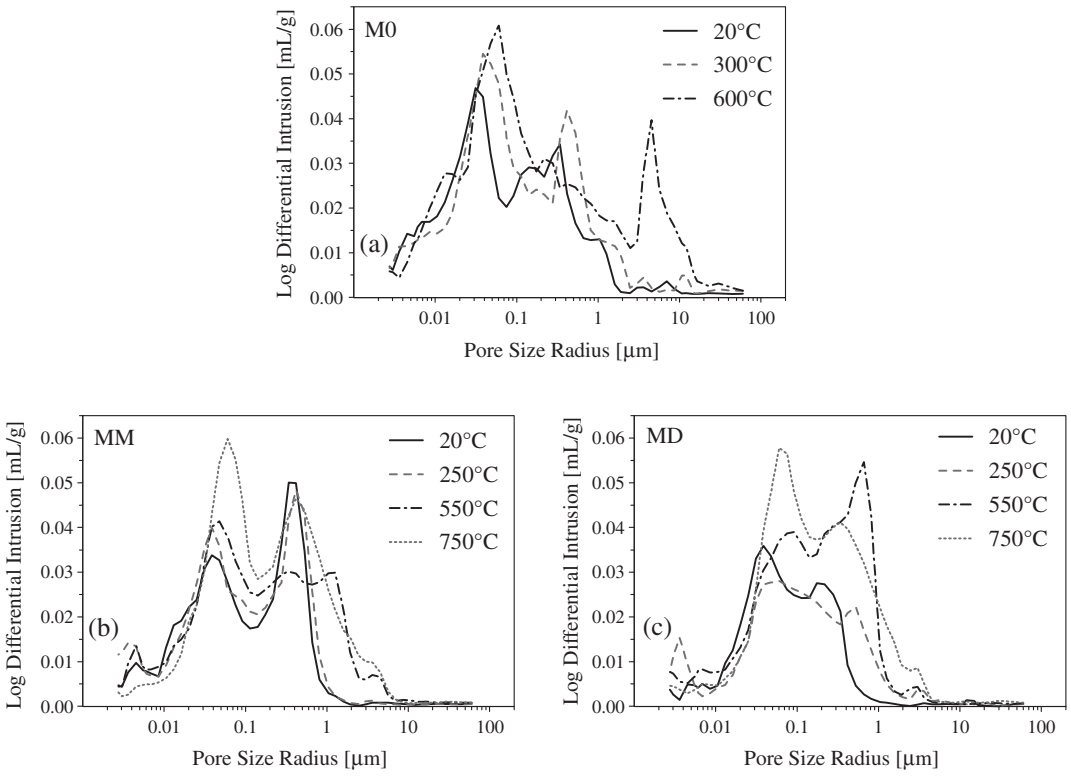

Fig. 7. Plots of the differential intrusion (in log scale), as a function of pore radius.

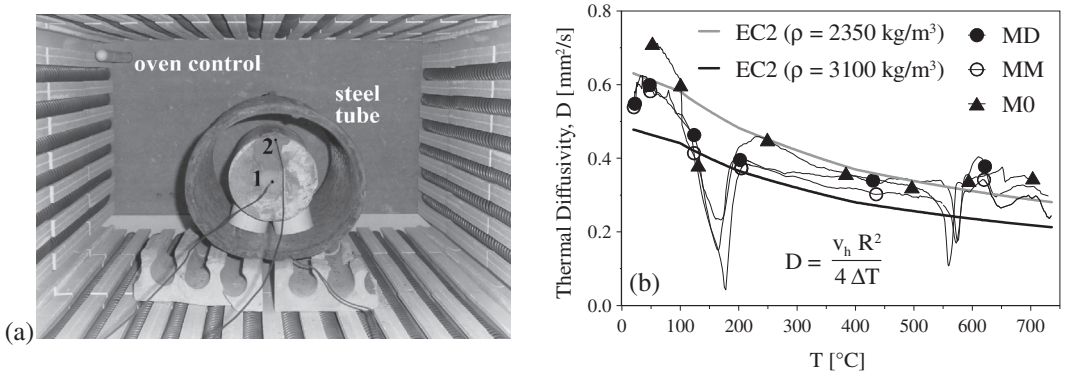

Fig. 8. Thermal diffusivity: typical specimen inside the oven (a); and baritic versus ordinary concrete (b); note that the two curves derived from EC2 are based on the lower curve given for the thermal conductivity.

(2300–2400 kg/m^3 at 20 °C for ordinary concrete – thin curve in Fig. 8b – and 3100 kg/m^3 for the heavy mixes considered in this study – thick curve in Fig. 8b).

In the range 250–500 °C, the curve corresponding to EC2 provisions is very well matched by the thermal diffusivity of Mix M0, as expected since M0 is an ordinary mix.

The sharp downward spikes at 150–200 °C and 550–580 °C are due to two endothermic phenomena: (a) the change of state of the water from liquid to vapor in the micropores, and (b) the change in the crystalline system (from α to β) of the quartz contained in the mixed aggregates.

The lower diffusivity of baritic concrete is mostly due to its higher mass per unit volume, since the thermal conductivity and specific heat exhibit similar reductions compared to ordinary concrete. (Hence the ratio between the thermal conductivity and the specific heat is pretty much the same in both ordinary and baritic concretes).

For instance, for $\lambda/\lambda_o = 0.66$ at 180–200 °C (mean value [9,11]), $c/c_o = 0.66$ [9] and $\rho/\rho_o = 1.32$ (as in this study), D/D_o is equal to 0.75 at 200 °C, with a decrease close to 25%, that agrees with the higher decrease indicated in [9] (= 38%) once the larger mass per unit volume in [9] (= 3700–3800 kg/m^3) is taken care of. (λ_o, c_o, D_o = thermal properties of ordinary concrete).

Summing up, the thermal diffusivity is roughly inversely proportional to the mass per unit volume, since both the thermal conductivity and the specific heat are decreasing functions of the temperature and their effects on the diffusivity tends to cancel each other.

8. Residual mechanical properties (after heating and cooling)

The stress–strain curves in compression are plotted in Fig. 9; all are characterized by well-defined linear loading branches, nonlinearities more or less pronounced close to the peak and rather

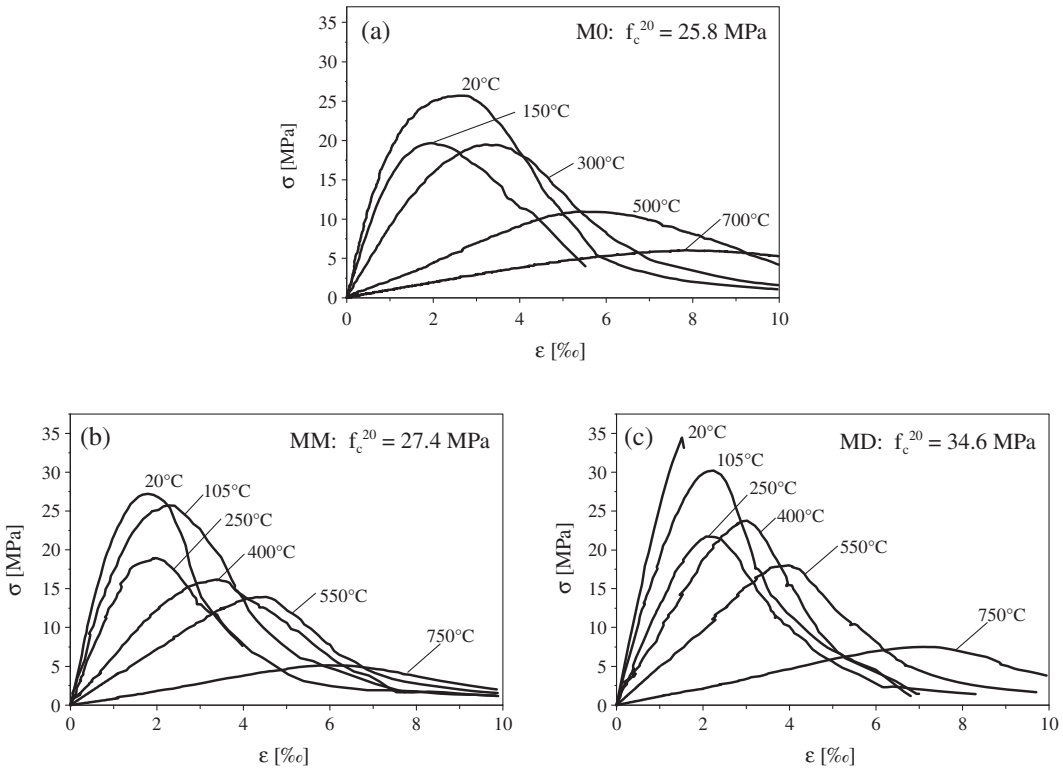

Fig. 9. Mean stress–strain curves in uniaxial compression: M0 (a), MM (b) and MD (c).

regular descending branches, that are an indication of the increasing toughness at any temperature at and above 105 °C. The stress–strain curves clearly show that the behaviors of Mixes MM (Fig. 9b) and MD (Fig. 9c) are more brittle than that of Mix M0 (Fig. 9a); Mix MD is not only the most brittle, but is also stronger than Mix MM at any temperature, as a consequence of the different aging conditions.

Contrary to Mix MM, Mix MD exhibits a partial strength recovery in the range 250–400 °C (Fig. 9c), something found also in Mix M0 in the range 150–300 °C, but in a weaker form (strength stabilization instead of strength recovery, Fig. 9a). This phenomenon – often found in ordinary cementitious mortars and concretes, but more likely to occur in high-performance and self-compacting concretes – may be explained as follows [27]: (a) delayed hydration (or *rehydration*) of the cement paste due to the heat-induced water migration in the pores under the driving force of pore pressure, as demonstrated by the decrease of anhydrous cement in SCC at high temperature; and (b) better bonding properties in the newly-formed hydration products. These two concurrent phenomena have the upper hand of the increasing porosity, that comes from the expulsion of the bound water at high temperature. (Note that the compressive strength may exceed even by 20% that of the virgin material).

The normalized plots of the strengths in compression and in indirect tension by splitting, as well as those of the ultrasonic velocity are reported in Figs. 10, 11 and 12, respectively.

Mix MM adheres to ACI curve for calcareous (or carbonate) concrete below 400 °C and exhibit the same trend as ACI curve for siliceous concrete above 400 °C ([28], Fig. 10a). Mix MM fits also very well EC4 [29] residual curves for either siliceous or calcareous concretes (Fig. 10b). The same can be said for Mix MD above 400 °C. As for the reference mix, Mix M0 behavior is half way between ACI residual curves for siliceous and calcareous concretes (Fig. 10a), but exhibits lower values than those corresponding to EC4 residual curves. On the whole, the good behavior of baritic concrete at high temperature comes from the closeness of the thermal expansion coefficients of the coarse aggregate and of the mortar, both based on barite (Fig. 1).

As expected, the tensile strength (Fig. 11) is more temperature-sensitive than the compressive strength, with no sizable differences between the two heavy mixes, whose behavior is slightly better than that of Mix M0 above 400 °C. The agreement with EC2 curve [25] in *hot* conditions (that is cited here as nothing similar is found in ACI) can be considered as satisfactory, provided that two facts are taken into account: firstly, the mechanical performance in *residual* conditions (as in the tests performed in this project) is always lower than that in *hot* conditions; and secondly, the indirect tensile strength by splitting tends to be larger than the direct tensile strength, thanks (a) to the stress redistribution taking place in the former case and (b) to the friction under the loading points. To what extent these two contradictory facts evolve with the temperature and counterbalance each other is still open to speculation.

As for the strain at the peak stress (Fig. 13a), the values are comprised between 1.5 and 1.8‰ at 20 °C (Mixes MD and MM), but the mean value for both mixes is close to 2‰ up to 250 °C; above this temperature, the strains jump to 6–7‰ at 750 °C. This trend is confirmed by Mix M0, whose strain at the peak stress is close to 2‰ up to 150 °C and then jumps to 7–8‰ at 700 °C. Summing up, the following bi-linear curves hold for ordinary and baritic concretes:

- *Ordinary concrete*: for $T \leqslant 175$ °C $\Rightarrow \varepsilon_{c1} = 2‰$;
  for $T = 175–750$ °C $\Rightarrow \varepsilon_{c1} = 2‰\ [1 + 5.57 \cdot 10^{-3}(T - 175)]$.
- *Baritic concrete*: for $T \leqslant 250$ °C $\Rightarrow \varepsilon_{c1} = 2‰$;
  for $T = 250–750$ °C $\Rightarrow \varepsilon_{c1} = 2‰\ [1 + 4.70 \cdot 10^{-3}(T - 250)]$.

The closeness of the heat sensitivity of the two heavy mixes to that of ordinary concrete is confirmed by the plots of the secant elastic modulus (Fig. 13b), where the envelope of the test results examined by Phan and Carino [30] is reported.

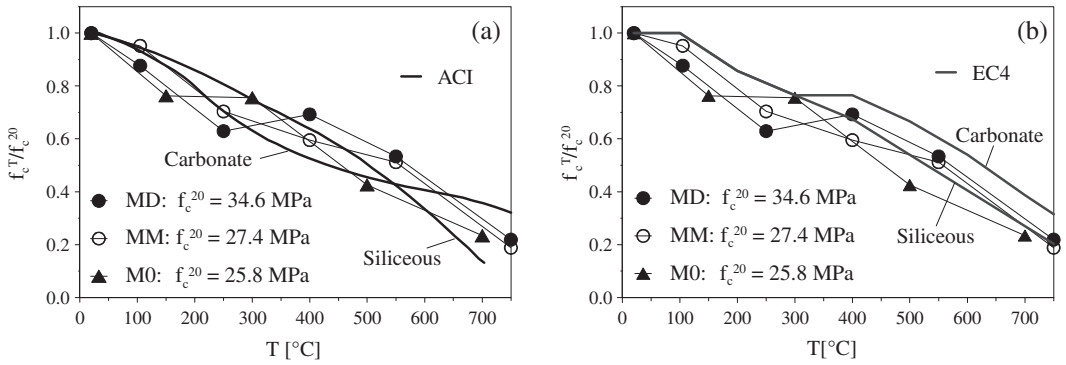

Fig. 10. Normalized plots of the residual compressive strength with ACI provisions (a) and EC4 provisions (b).

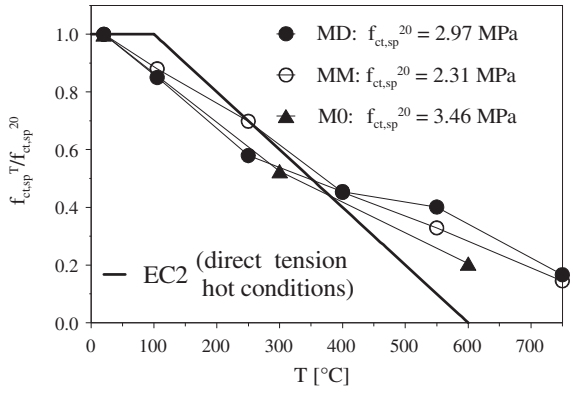

Fig. 11. Normalized plots of the tensile strength by splitting.

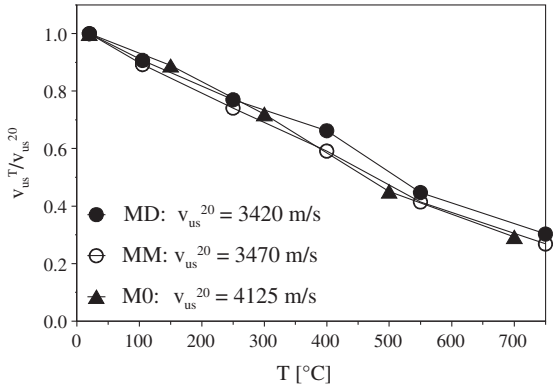

Fig. 12. Plots of the normalized ultrasonic velocity measured along the axis of the specimens, as a function of the temperature.

Similarly to the normalized strengths in compression and tension (Figs. 10 and 11), the normalized elastic modulus is a bit more heat-sensitive in Mix MD up to 250–350 °C, but on the whole the two heavy mixes and the reference mix have very similar behaviors, with rather low values for the secant moduli compared to the values provided by EC2 for ordinary concrete in virgin conditions (E_c = 11,000 $f_c^{0.3}$ MPa). As a matter of fact, looking at Table 2 the secant moduli of Mixes MM, MD and M0 are from 17% to 20% lower than the values predicted by the previous equation. (It should be observed, however, that differences up to ±20% with respect to EC2 are rather often found). In the case of the two heavy mixes, such low values are hardly explainable, unless they are due to the rather low hardness of barite (3–3.5 in the Mohs scale compared with 3.5–7 for the minerals found in commonly-used calcareous and siliceous aggregates) and to its rather microfractured structure [9].

Similar low values were found by Witte and Backstrom (−20% [9]), Crispino (−19% [11]) and Sakr and El-Hakim (−12% [12]). Much higher values were found for the dynamic modulus by Topçu [14] and Kilincarslan et al. [15], while the values derived from the stress–strain curves by Topçu [14] are very low.

9. Damage indices

Load-induced damage in quasi-brittle materials – mainly in the form of microcracking – can be quantified by means of *damage indices*, generally indicated with D (D = 1 = fully-damaged material or failure of the material; D = 0 = no damage in the material). Damage indices were first proposed in the seventies of the past century; among the parameters controlling the damage, the elastic modulus, the density, the ultrasonic velocity, the stress amplitude, the strain rate and the hardness were introduced by various researchers [31], to describe the effect of loading on materials stiffness, ductility, creep behavior and low-/high-cycle fatigue resistance.

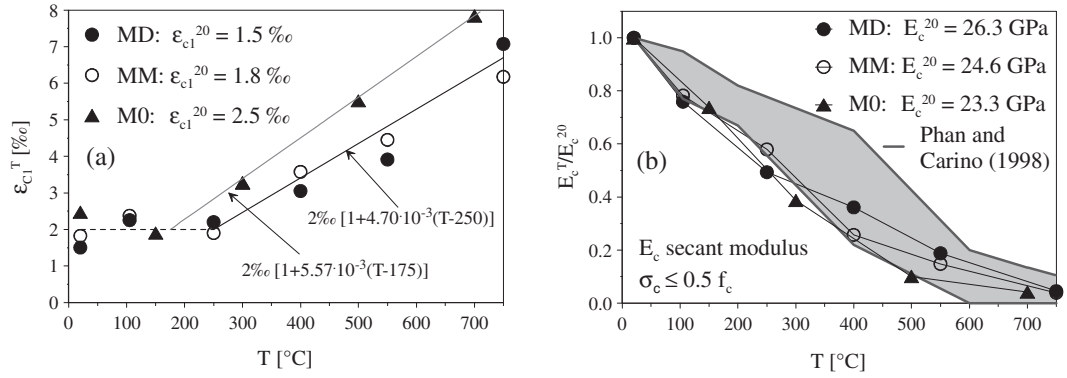

Fig. 13. Plot of the strain at the peak stress (a); and normalized plots of the secant elastic modulus (b).

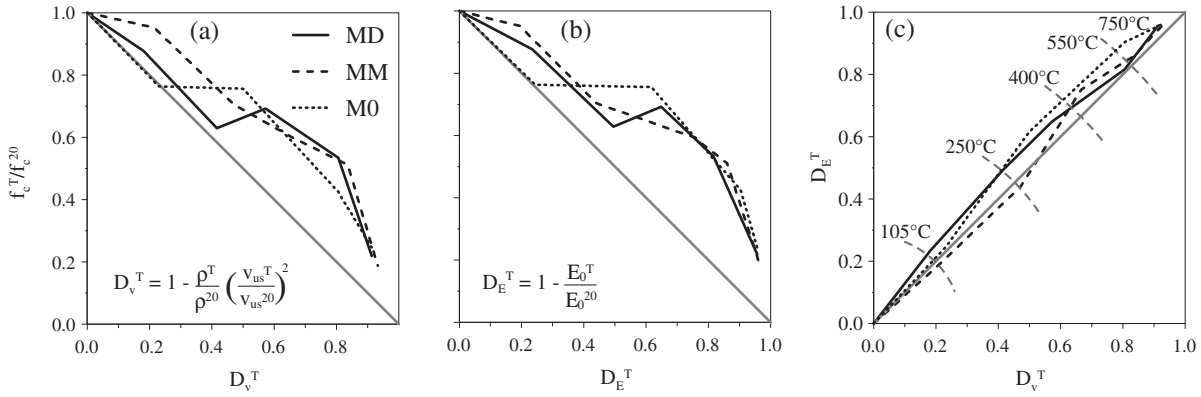

Fig. 14. Plots of the damage indices based on the ultrasonic velocity (a); and on the Young's modulus (b); and correlation between the two indices, for various values of the temperature (c).

In the case of heat-damaged concrete (where the damage comes mostly in the form of microcracking, extraporosity and chemo-physical changes), the indices based on the elastic modulus [32,33] (D_E^T, Eq. (2)) and on the ultrasonic pulse velocity ($\widetilde{D}_v^T$, Eq. (3)) are used:

$$D_E^T = 1 - \left(E^T/E^{20}\right) \tag{2}$$

$$\widetilde{D}_v^T = 1 - \left(v_{us}^T/v_{us}^{20}\right)^2 \tag{3}$$

where E and v_{us} are the elastic modulus and the ultrasonic pulse velocity, respectively; note that both v_{us}^T and E^T are decreasing functions of the temperature (Figs. 12 and 13b).

Since in an elastic continuum the elastic modulus is proportional to the square of the velocity of the ultrasonic waves times the mass per unit volume ρ, the damage index based on the ultrasonic velocity can be reformulated as follows:

$$D_v^T = 1 - \left(\rho^T/\rho^{20}\right) \cdot \left(v_{us}^T/v_{us}^{20}\right)^2 \tag{4}$$

Note that in a perfectly elastic continuum (E^T/E^{20}) and [$(\rho^T/\rho^{20}) \cdot (v_{us}^T/{v_{us}}^{20})^2$] coincide (should the dependence of the Poisson ratio on the temperature be neglected), while in an actual (inelastic) continuum the results are more or less different, depending on the definition of E. (Slope E_0 of the stress–strain curve at the origin; E_{st} = stabilized modulus after a number of load cycles; E_c = first-loading secant modulus; here the modulus is introduced as E_0, that is a function of the temperature).

In the specific case of heat-damaged materials and structures, quantifying the mechanical damage through the formulation given in Eq. (4) is more handy and precise than by using the formulation given in Eq. (2), for at least three reasons:

- Eq. (2) requires the extraction of cores to measure E^T and E^{20}, while Eq. (4) requires the measurement of the ultrasonic velocity, that introduces no-further damage in the heat-affected material or structure.
- The correlation between the normalized ultrasonic velocity and the temperature is less material-dependent than that of the elastic modulus (see Figs. 12 and 13b, where both quantities are normalized).
- The correlation between the index based on the ultrasonic velocity and the compressive strength is better than that of the index based on the elastic modulus (Figs. 14a and b).

So, measuring the damage through the ultrasonic velocity is a powerful means to compare different mechanical behaviors within the same fire scenario, or the behaviors of a given structural member within different fire scenarios, or even to evaluate the compressive strength (Fig. 14a) or the elastic modulus (by equating Eqs. (2) and (4)).

Furthermore, comparing the two indices (Fig. 14c) gives information on the capability of a heat-damaged material to retain its initial linear behavior. From this view point, the two heavy Mixes MD and MM behave slightly better than the ordinary Mix M0 (dotted curve), as indicated by the closeness of the continuous and dashed curves to the bisector (one-to-one correlation).

Furthermore, between the two heavy mixes, Mix MM (cured in moist conditions) has a better and more definite linear behavior at least up to 300–350 °C.

10. Conclusions

The results of this study show that baritic concrete is as resistant to high temperature as ordinary concrete, and has better insulation properties mostly because of its higher mass per unit volume.

Stress–strain curves in compression

Both in virgin and residual conditions, at any temperature the curves exhibit a well defined linear ascending branch, with the strain at the peak close to 2‰ at room temperature, and to 6–8‰ at 750 °C, as in ordinary concrete; the descending branches become increasingly softer at high temperature.

Strength and stiffness

Baritic concrete is slightly less temperature sensitive than ordinary concrete in terms of compressive strength above 400 °C, but the overall behavior is not very different from that predicted by ACI and European curves for siliceous and carbonate (calcareous) aggregates; the tensile strength and the elastic modulus are more affected by the temperature; however, below 300 °C the values of the elastic modulus are close to the lowest found in the literature for ordinary concrete, while above 400 °C they are close to the mean values found in the literature. As should be expected, the concrete kept in moist conditions exhibits a somewhat lower mechanical performance at any temperature; the normalized decay, however, is practically the same for the mixes cured in different environments.

Mass loss, thermal diffusivity and porosity

Because of the greater mass of aggregate (that is very stable at high temperature), the mass loss of baritic concrete is smaller than that of ordinary concrete (a few percents less up to 750 °C), while the thermal diffusivity is lower than in ordinary concrete at any

temperature up to 750 °C. (The mass per unit volume is the controlling factor, since the effects of the thermal conductivity and of the specific heat tend to cancel each other, both quantities being decreasing functions of the temperature). As for the porosity, in spite of barite microfractured nature the two baritic concretes examined in this project have a porosity that is very similar to that of ordinary concrete, at any temperature; at high temperature, however, the pore-size radius tends to increase less in baritic concrete than in ordinary concrete.

Heat-induced damage

The heat-induced damage – mainly in the form of microcracking and increasing porosity – is effectively described by two *damage indices*, the first based on the velocity of the ultrasonic waves and the density, and the second based on the elastic modulus. The two indices – that coincide in any perfectly linear-elastic material – do not coincide in heated concrete, mostly because of the heat-induced damage and resulting non-linearities. However, the index based on the ultrasonic velocity appears to be more reliable, because of its slightly better correlation with the heat-affected compressive strength in both ordinary and heavy concretes. In addition, the roughly one-to-one correlation between the two indices makes it possible to evaluate – even in situ – the residual elastic modulus through the measurement of the ultrasonic velocity. Further studies on uniaxial compression at high temperature, as well as on multiaxial stress states and pre-loaded concrete during the heating process may be useful. However, the findings of this project and the limited results available in the literature confirm and extend to high temperature the conclusion of Witte and Backstrom, that baritic concrete compares favorably with any ordinary concrete containing good-quality aggregate, even if the former has the edge over the latter at high temperature.

Acknowledgements

The authors express their gratitude to Cinzia Provenzi and Umberto Ruspa, who performed most of the tests in partial fulfillment of the requirements concerning their BS Degree in Civil Engineering.

MS Eng. Pierumberto Perucchini and Dr. Fabio Erba of Beton Technology (Cavallasca, Como, Italy) are thanked for providing first-hand information on baritic concrete, as well as on its technology and behavior. The authors are also grateful to Dr. Patrick Bamonte of DICA – Politecnico di Milano, for his technical assistance and for providing the specimens, that were cast by Lombarda Calcestruzzi s.r.l. (Milan, Italy).

References

[1] Hilsdorf HK, Kropp J, Koch HJ. The effects of nuclear radiation on the mechanical properties of concrete. ACI – Am Concr Inst SP 55. Concr Concr Struct. Detroit, Michigan; 1978. p. 223–54.
[2] Bamonte P, Gambarova PG. Properties of concrete required in nuclear power plants. In: Hsu Thomas TC, Wu Chiun-Lin, Lin Jui-Liang, Lin Jui-Liang, editors. Infrastructure systems for nuclear energy. John Wiley and Sons, Ltd.; 2014. p. 409–38.
[3] Bouniol P. Bétons Spéciaux de Protection. Techniques de l'Ingénieur – Génie Nucléaire, BN 3 740; 2001. p. 29.
[4] Vodák F, Vydra V, Trtík K, Kapičková O. Effect of gamma irradiation on properties of hardened cement paste. RILEM – Mater Struct 2011;44:101–7.
[5] Vecchio FJ, Sato JA. Drop, fire and thermal testing of a concrete nuclear fuel container. ACI – Struct J 1998;85-S35:374–83.
[6] Taglioni A, Castellani A, Collepardi M, Pellegrini A, Pizzigalli G. Hazardous-waste containers in cementitious materials: leakage tests on small-scale specimens and on full-scale prototype. In: Politecnico di Milano, Italcementi, editors. Studies and researches 27. Brescia, Italy: Starrylink Pub. Co.; 2007. p. 11–30.
[7] Corps of Engineers – US Army. High-strength high-density concrete. US Army Engineer Waterways Experiment Station – Vicksburg (Mississippi, USA), Tech. Report No.6-635; 1963. p. 65.
[8] Shirayama K. Properties of radiation shielding concrete. ACI – J Am Concr Inst 1963;60(2):263–79.
[9] Witte LP, Backstrom JE. Properties of heavy concrete made with barite aggregates. ACI – J Am Conc Inst 1954;26(1):65–88.
[10] Weigler H, Fischer R. Influence of high temperatures on strength and deformations of concrete. ACI – Am Concr Inst SP 34-26. Concr Nucl Reactors; 1972. p. 481–94.
[11] Crispino E. Studies on the technology of concretes under thermal conditions. ACI – Am Concr Inst SP 34-25. Concr Nucl Reactors; 1972. p. 443–80.
[12] Sakr K, El-Hakim E. Effect of high temperature or fire on heavy-weight concrete properties. Cem Concr Res 2005;35:590–6.
[13] Revuelta D, Alonso MC, García JL, Barona A. Experimental study on a barite heavyweight self-consolidating concrete. ACI – Am Conc Inst SP 261-7. Recent Adv Concr Technol Sustainability Issues; 2009. p. 101–14.
[14] Topçu IB. Properties of heavyweight concrete produced with barite. Cem Concr Res 2003;33(6):815–22.
[15] Kilincarslan S, Akkurt I, Basyigit C. The effect of barite rate on some physical and mechanical properties of concrete. Mater Sci Eng, A 2006;424(1–2):83–6.
[16] Mather K. High-strength high-density concrete. ACI – J Am Concr Inst Title 62–56 Proc 1965(62):951–62.
[17] Behnood A. Effect of high temperatures on high-strength concretes incorporating copper-slag aggregate. Proc 7th Int Symp Utilization High-Strength/High-Perform Concr – ACI – S.P. 228 II. Washington D.C., USA; 2005. p. 1063–74.
[18] Kan YC, Pei KC, Chang CL. Strength and fracture toughness of heavy concrete with various iron aggregate inclusions. Trans. SMiRT 16. Washington D.C., USA. Paper 1230; 2001. p. 7.
[19] Bouniol P, Aspart A. Disappearance of oxygen in concrete under irradiation. The role of peroxides in radiolysis. Cem Concr Res 1998;28(11):1669–81.
[20] Lo Monte F, Bamonte P, Gambarova PG. Mechanical and thermal properties of a heavy radiation-proof concrete exposed to high temperature. Proc 7th Int Conf Concr Under Severe Conditions – CONSEC 13. Nanjing, China, September 23–25, vol. 2; 2013. p. 1672–84.
[21] Lo Monte F, Bamonte P, Gambarova PG. Physical and mechanical properties of heat-damaged structural concrete containing expanded polystyrene syntherized particles. Fire Mater J 2014. http://dx.doi.org/10.1002/fam.2230.
[22] Bažant ZP, Kaplan MF. Concrete at high temperatures: material properties and mathematical models. Concr Des Construction Ser. Longman Group Ltd.; 1996. p. 412.
[23] Felicetti R, Gambarova PG. Effects of high temperature on the residual compressive strength of siliceous HSCs. ACI – Mater J 1998;95(4):395–406.
[24] European Norm EN 12390-6. Testing hardened concrete – Part 6: tensile splitting strength of test specimens. ICS 91.100.30; 2009. p. 11.
[25] EN 1992-1-2:2004. Eurocode 2 – design of concrete structures – part 1–2: general rules – structural fire design. European Committee for Standardization (CEN), Brussels (Belgium).
[26] Felicetti R. Assessment of the equivalent thermal diffusivity for fire analysis of concrete structures. Proc Fib Task Group 4.3 Workshop. Fire Des Concr Struct. Coimbra, Portugal, November 8–9, 2007; 2008. p. 149–58.
[27] Fares H, Noumowé A, Remond S. Self-consolidating concrete subjected to high temperature: mechanical and physico-chemical properties. Cem Concr Res 2009;39:1230–8.
[28] ACI 216-1.07. Code requirements for determining fire resistance of concrete and masonry construction assemblies. Report by Joint ACI/TMS Committee 216; 2007. p. 32.
[29] EN 1994-1-2:2004. Eurocode 4 – design of composite steel and concrete structures – part 1–2: general rules – structural fire design. European Committee for Standardization (CEN), Brussels (Belgium).
[30] Phan LT, Carino NJ. Review of mechanical properties of HSC at high temperature. ASCE – J Mater Civ Eng 1998;10(1):58–64.
[31] Lemaître J. A course on damage mechanics. Springer Verlag; 1992.
[32] Di Prisco M, Felicetti R, Gambarova PG. On the evaluation of the characteristic length in high-strength concrete. In: Azizinamini A, Darwin D, French C, Kona, editors. Proc Int Conf High-Strength Concr – ASCE. Hawaii, USA; 1997. p. 377–90.
[33] Bamonte P, Felicetti R. High-temperature behaviour of concrete in tension. Struct Eng Int, Assoc Bridge Struct Eng – IABSE 2012;22(4):493–9.